Arch. Metall. Mater. **63** (2018), 4, 1663-1672

DOI: 10.24425/amm.2018.125091

A. LISIECKI*# A. KURC-LISIECKA**

AUTOMATED LASER WELDING OF AISI 304 STAINLESS STEEL BY DISK LASER

The automated laser welding process of 2.0 mm thick sheets of AISI 304 stainless steel was investigated. The disk laser with a beam spot diameter of 200 μm was used for bead-on-plate and next for autogenous butt joints welding. The influence of basic welding parameters such as laser power, welding speed, and focal spot position on fusion zone configuration, quality of joints, microstructure changes, and microhardness distribution across the joints were analysed and presented in this paper. The results have shown that stiffening of the 2.0 mm thick sheets is crucial for providing high quality and reproducibility of butt joint in a case of AISI 304 stainless steel due to relatively low thermal conductivity and simultaneously high thermal expansion. Relevant drop of microhardness in the weld zone was observed. The mean value of microhardness of the base metal was 230 HV0.1, while the microhardness in fusion zone of the test welds was ranged from 130 to 170 HV0.1. Additionally the microstructure changes in the weld metal and also in the heat affected zone of test joints is described.

Keywords: autogenous laser welding, butt joints, stainless steel, AISI 304, austenitic steel

1. Introduction

Modern chrome-nickel type stainless steels are widely used in almost all branches of industry such as chemical, gas, petroleum, food processing, automotive, aerospace, nuclear or even cryogenic application [1-5]. Among stainless steels, the austenitic stainless steels (ASS) having face-centred cubic structure (fcc) and different characteristics such as weldability, corrosion resistance, and mechanical properties are about 70% [3-7]. The most popular in this group is the AISI 304 stainless steel containing 18% of chromium and 8% of nickel with austenitic structure. The AISI 304 has potentially wide range of application because of satisfactory corrosion resistance, good formability, and high mechanical properties such as high ultimate strength, high yield point, high strength/weight ratio, and at the same time high ductility [1-3,8-12].

The austenitic AISI 304 stainless steel exhibits good weldability and variety welding processes can be applied for joining of components made of this steel. For example, high quality joints of austenitic AISI 304 stainless steel are produced by electric resistance welding, fusion arc welding or electron beam welding [1,13-15]. The AISI 304 stainless steel with a typical chemical composition required by the standard is characterized by a stable single-phase austenitic structure. However, in a case of lower content of nickel (below 8%) the structure may be unstable, and under high cooling rates a small content of a ferrite delta may occur also. Due to single-phase austenitic structure, lower thermal conductivity compared to mild steel, and higher thermal expansion coefficient, low heat input of welding is recommended in a case of such type of steel. Single-phase austenitic steels are susceptible for hot cracking during welding [16,17]. Moreover, efficient protection of the welded region must be provided to avoid the harmful influence of gases in the ambient air [18-20].

The continuous development of laser generators and laser welding devices allows also the development in the field of laser welding technology [8,21]. Lasers as a heat source are attractive for joining of austenitic stainless steels because they provide high power density thanks to focusing the laser beam into very small spot, usually 100÷300 μm in diameter, and thus high penetration depth, high welding speed, and thus low heat inputs [22,23]. Particularly noteworthy are the new generations of solid state lasers such disk lasers and fiber lasers [1,15,24]. They provide very high output power at low beam divergence, flexibility of beam delivery by fiberglass, and also very high efficiency [24-26]. However, elaboration of welding technology and putting it into practice requires investigations of the influence of welding parameters and welding conditions on the course of welding process and on the performance of the joints [1,15,27,28].

Therefore, investigations on automated laser welding of butt joints of AISI 304 stainless steel were undertaken using a solid state disk laser. The influence of basic laser welding parameters on shape, quality, microstructure, and microhardness distribution was analysed.

* SILESIAN UNIVERSITY OF TECHNOLOGY, FACULTY OF MECHANICAL ENGINEERING, DEPARTMENT OF WELDING ENGINEERING, 18A KONARSKIEGO STR., 44-100 GLIWICE, POLAND
** WSB UNIVERSITY IN POZNAŃ, FACULTY OF WSB UNIVERSITY IN CHORZÓW, SCIENTIFIC INSTITUTE OF ENTREPRENEURSHIP AND INNOVATION, DEPARTMENT OF MANAGEMENT ENGINEERING, 29 SPORTOWA STR., 41-506 CHORZÓW, POLAND

Corresponding author: aleksander.lisiecki@polsl.pl

2. Materials and experimental procedure

The samples for welding tests were laser cut from a 2.0 mm thick sheet of AISI stainless steel at delivery conditions into coupons 100 mm long and 40 mm wide. The AISI 304 steel is chrome-nickel type steel characterized by satisfactory corrosion resistance and austenitic microstructure in general. The chemical composition determined for the investigated AISI 304 steel is given in Table 1. The welding trials were conducted by means of a fully automated stand composed of a disk laser generator with maximum output power of the laser beam up to 3.3 kW, a laser welding head coupled with the generator by a fiberglass with 200 μm core diameter, a 3D positioning system, clamping devise with root protection gas nozzle, and automated shielding gas delivery system. The samples to be welded were fixed and stiffened in a clamping device which was mounted on the table below the laser head. All the process parameter, as well as the sample movement were controlled by the CNC system. Shielding gas argon was delivered to the weld region by cylindrical nozzles 10 mm in diameter prior to the welding and the flow rate was kept constant at 12 l/min. At the beginning stage of the study bead-on-plate welding tests were done in a wide range of welding parameters in order to determine the welding conditions that allow to provide a full penetration and a narrow weld at relatively low heat inputs, Table 2. Both the bead-on-plate and butt joints welding tests were conducted as autogenous laser welding by melting of the sheets and edges to be welded. Beside the top weld region protection additionally root shielding was applied by argon flow via longitudinal nozzle at 5 l/min. After the initial tests of bead-on-plate welding the parameters considered as optimal were chosen for laser welding of real butt joints. The quality of bead-on-plate welds and butt joints was evaluated by visual inspection, macrographs and micrographs observation by light microscopy and also the Vickers microhardness measurements on the across sections were done according to PN-EN ISO 6507-1 standard. The cross sections were prepared by grinding and subsequent polishing by diamond suspension of 6 μm, 3 μm, and 1 μm respectively. The microstructure was revealed by etching in the reagent composed of iron chloride $FeCl_3$, hydrochloric acid HCl, and water H_2O, in proportions 1:1:4. Regions of base metal (BM), heat affected zone (HAZ), and weld metal (WM) were observed and analysed. Results of the study are presented in Figs. 1-15 and Table 2.

TABLE 1

Chemical composition of the investigated 2.0 mm thick sheet of AISI 304 stainless steel

Concentration of elements, wt.%								
C	Cr	Ni	Mn	Si	P	S	Mo	Fe
0.02	18.07	7.8	1.31	0.39	0.03	0.004	0.25	rest

TABLE 2

Parameters of bead-on-plate welding and butt joints welding of 2.0 mm thick sheets of AISI 304 stainless steel using disk laser Trumpf TruDisk 3302

Bead No.	Output power, kW	Welding speed, m/min	Energy input, J/mm	Focal spot position, mm	Remarks
1	1.0	0.5	120	0	UF, EFR
2	1.0	1.0	60	0	SF, EP, C
3	1.0	1.5	40	0	ERR, EC
4	1.0	1.5	40	+1	EC, SF
5	1.0	1.5	40	–1	UC, SP
6	1.0	1.5	40	–1.5	SF, ERR
7	1.0	2.0	30	–1	UC, SP
8	1.0	3.0	20	–1	UC, SP
9	1.5	4.0	22.5	–1	UC, SP

Other parameters: Shielding gas Ar, flow rate of shielding gas from the weld face side; 12 l/min, from root side; 5 l/min, laser beam spot diameters; 200 μm,

Quality assessment; UF – uneven face, EFR – Excessive weld face reinforcement, SF – Smooth weld face, C – crater, EC – Excessive convexity, EP – excessive penetration, ERR – excessive root reinforcement, UC – undercut, SP – spatter

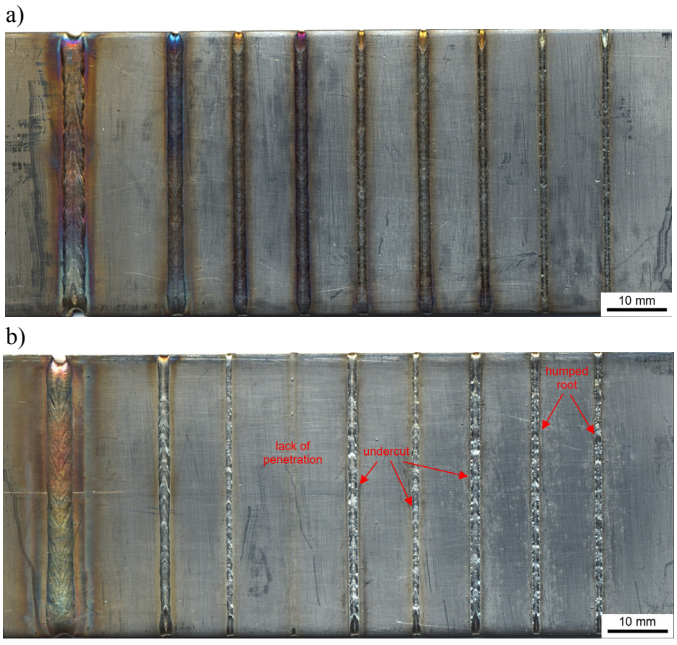

Fig. 1. A view of the bead-on-plate welds produced by disk laser melting of 2.0 mm sheet of AISI 304 stainless steel (bead No. 1 to 9 from left, Table 3); a) weld face; b) root surface

3. Results and discussion

As can be seen in Fig. 1, the surface of bead-on-plate welds both on the face and root is smooth and even in a case of welds produced at the focal spot set on the top surface of the sheets, Table 2. In other cases surfaces from the root side are humped with slight but clear undercuts, Fig. 1. Moreover, in a case of the bead No.4 produced at the focal spot set 1.0 mm over the top surface, lack of penetration of 2.0 mm thick sheet occurred. Thera are no traces of spatter on the surfaces of the sample after bead-on-plate laser welding. In a case of the butt joints the highest quality determined during visual inspection was exhibited by the joint No.1 welded at output power 1.0 kW, welding speed

2.0 m/min, and focal spot set 1.0 mm below the top surface (set of parameters No. 7, Table 2), Fig. 2. In the case of the two other test joints some imperfections such as humping, incomplete penetration and fusion, uneven face, Figs. 3,4.

Observations of macrostructure of the bead-on-plate welds revealed single pores in root region for the bead No. 3, 4 and also in the middle region for the bead No. 1, Figs. 5,7,9. The porosity of weld metal is a typical problem during laser welding

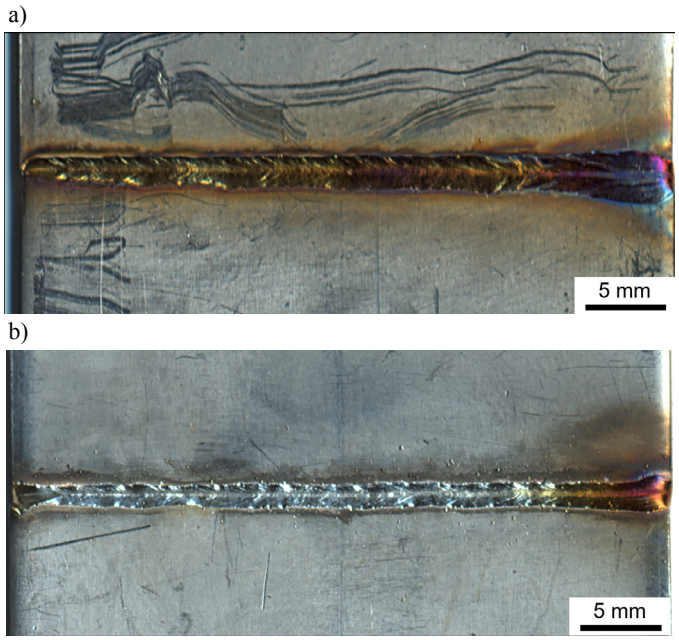

Fig. 2. A view of the butt joint of 2.0 mm sheet of AISI 304 stainless steel laser welded by the disk laser at output power 1.0 kW, welding speed 2.0 m/min, and focal spot position –1.0 mm (Table 3); a) weld face, b) root surface

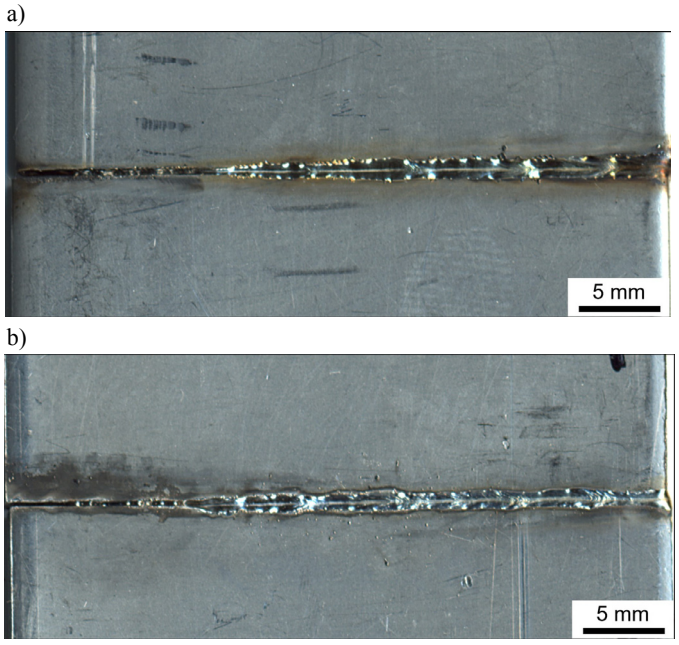

Fig. 3. A view of the butt joint of 2.0 mm sheet of AISI 304 stainless steel laser welded by the disk laser at output power 1.0 kW, welding speed 3.0 m/min, and focal spot position –1.0 mm (Table 3); a) weld face, b) root surface

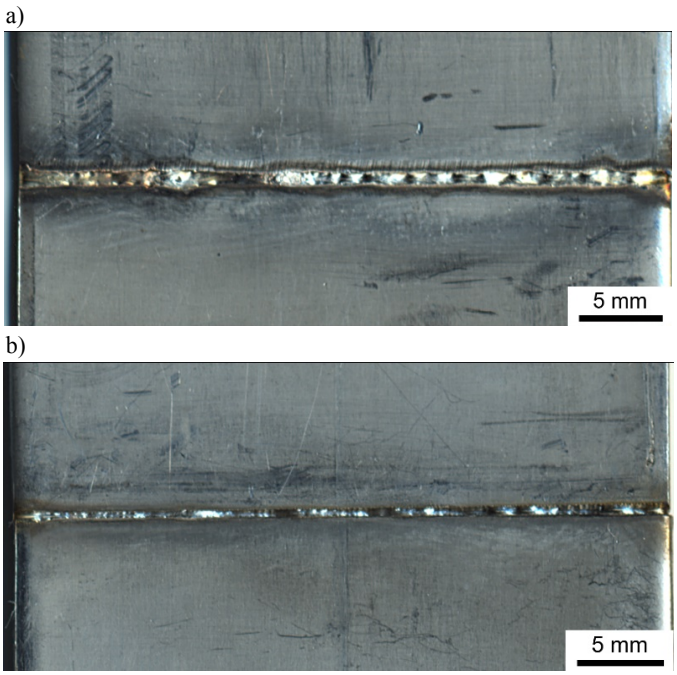

Fig. 4. A view of the butt joint of 2.0 mm sheet of AISI 304 stainless steel laser welded by the disk laser at output power 1.5 kW, welding speed 4.0 m/min, and focal spot position –1.0 mm (Table 3); a) weld face, b) root surface

at the keyhole mode, when high power density of the laser beam causes partial evaporation of the irradiated metal. The tendency to formation of pores is related to the stability of the keyhole. When the keyhole is unstable the vapours of the welded metal may be trapped inside the keyhole. To eliminate the porosity caused by the instability of the keyhole, precise selection of laser welding parameters is required. As can be seen, the shape of the fusion zone and also the depth/width ratio of the welds depend strongly on the welding parameters and conditions. Influence of the welding speed on the weld shape is illustrated in the case bead-on-plate welds from 1 to 3. Those beads were produced at constant output power of 1.0skW, focal spot set on the top surface of sheets to be welded, and different welding speed, Table 2, Fig. 5. The weld shape is changed from wide columnar for the bead produced at the lowest welding speed of 0.5 m/min thus the highest energy input of 120 J/mm, to the shape in X configuration (hourglass like shape) for the bead produced at medium welding speed of 1.0 m/min and also medium energy input of 60 J/mm, up to the shape in T configuration (mushroom like shape) for the bead produced at the highest welding speed of 1.5 m/min and energy input of 40 J/mm, Fig. 5. For comparison the depth/width ratio for the bead-on-plate welds is 0.5 for the bead produced at energy input of 120 J/mm, 0.86 for the bead produced at energy input of 60 J/mm, and 1.17 for the bead produced at energy input of 40 J/mm, Fig. 6. In turn, the influence of focal spot position on the penetration depth, shape, and depth/width ration is illustrated in the case bead-on-plate welds from 3 to 6. Those beads were produced constant output power of 1.0 kW, welding speed of 1.5 m/min, thus constant energy input 40 J/mm, Table 2. As can be seen, rising the focal plane over the top

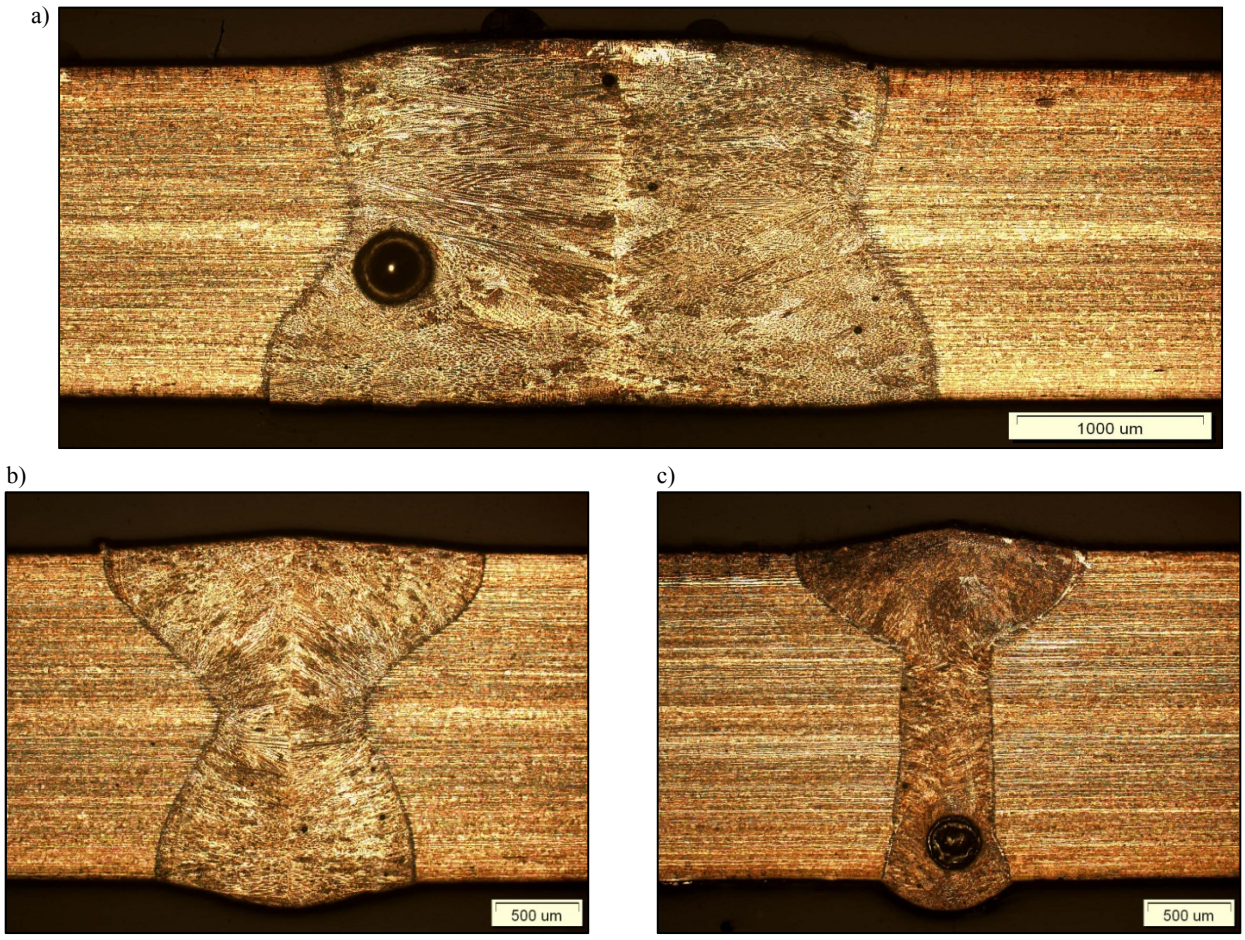

Fig. 5. Macrostructure on cross sections of the simulated welds produced on AISI 304 steel sheets 2.0 mm thick by bead-on-plate laser welding at 1.0 kW of output power and different welding speed (Table 3); a) 0.5 m/min, b) 1.0 m/min, c) 1.5 m/min

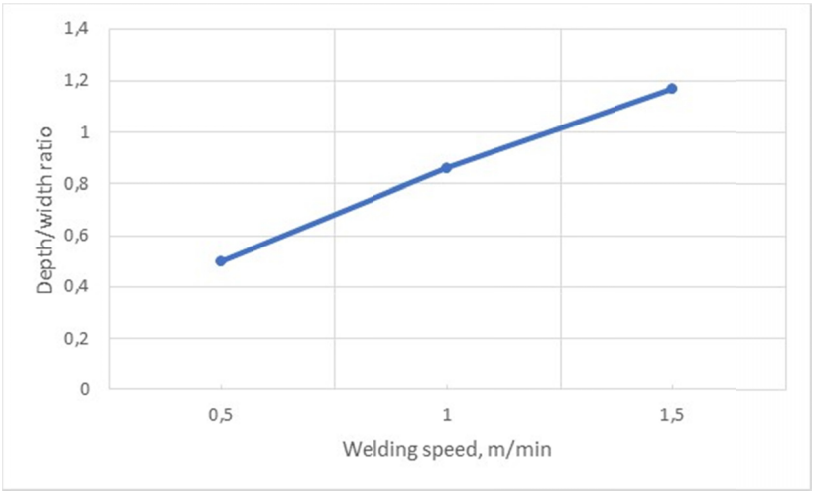

Fig. 6. Influence of the welding speed on the depth/width ratio of the weld during bead-on-plate laser welding of 2.0 mm thick sheet of AISI 304 stainless steel at constant laser beam output power 1.0 kW and focal spot set on the top surface of the sheets to be welded, Table 3

surface of the sheet at the distance of 1.0 mm resulted in lack of penetration for the 2.0 mm thick sheet but the T configuration of the bead was maintained, Figs. 5,7,8. On the other hand, setting the focal plane 1.0 mm below the top surface of the sheet resulted in clear change in the shape to double-T configuration (dumbbell like shape), Fig. 7b. Further decreasing the focal plane to 1.5 mm below the top surface caused another change in shape to T configuration, Fig. 7c,8. In a case of autogenous, single pass welding the double-T configuration of the fusion zone is favorable for providing the proper geometry and quality of the weld face and root. Therefore, next three bead-on-plate welds were produced at such focal spot position and lower energy inputs as a result of increasing the welding speed, Table 2. The shape configuration of the beads produced at the focal spot set 1.0 mm below the

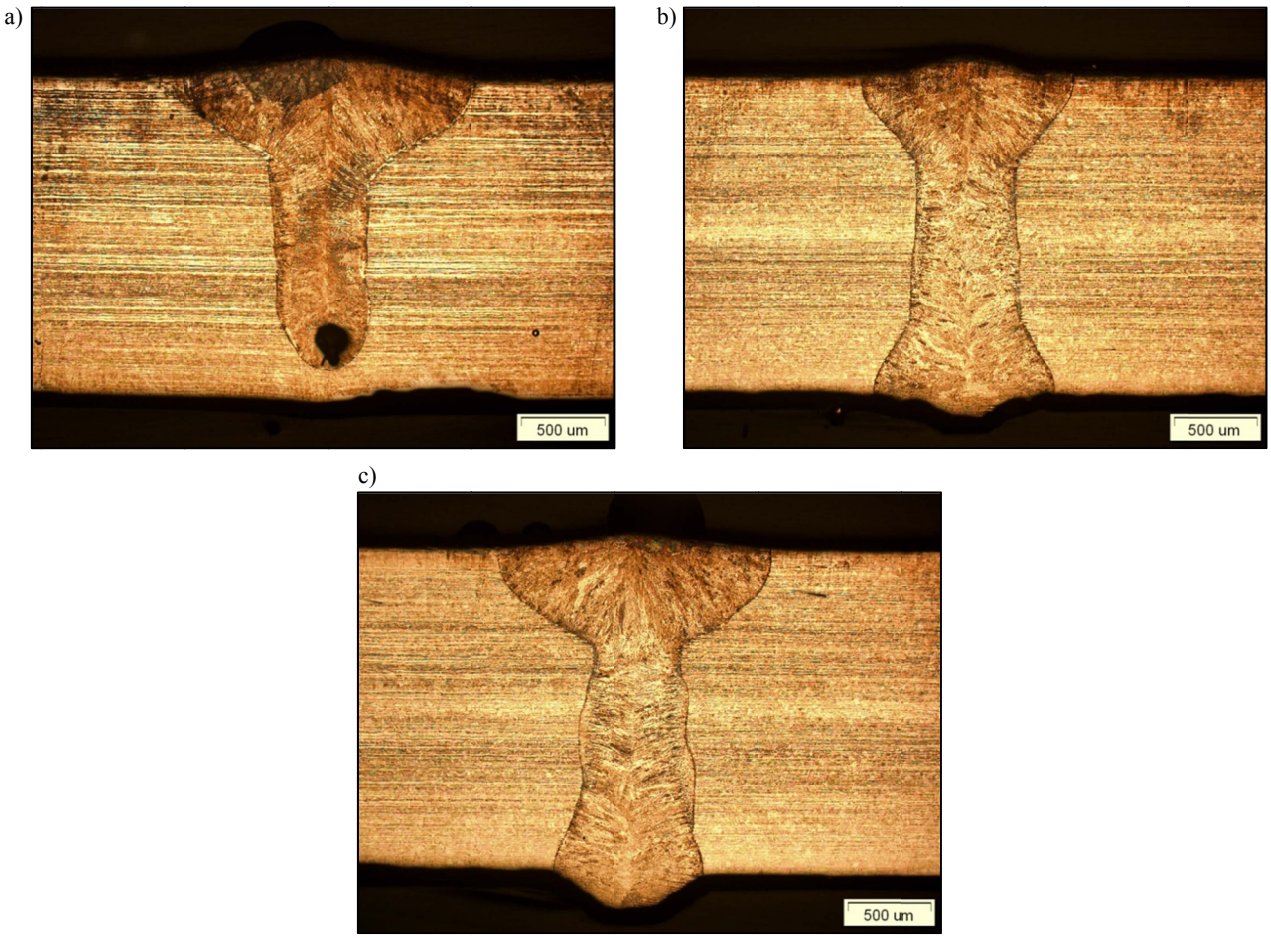

Fig. 7. Macrostructure on cross sections of the simulated welds produced on AISI 304 steel sheets 2.0 mm thick by bead-on-plate laser welding at 1.0 kW of output power, welding speed 1.5 m/min, and different focal spot positions (Table 3); a) 1 mm over the top surface, b) 1 mm below the top surface, c) 1.5 mm below the top surface

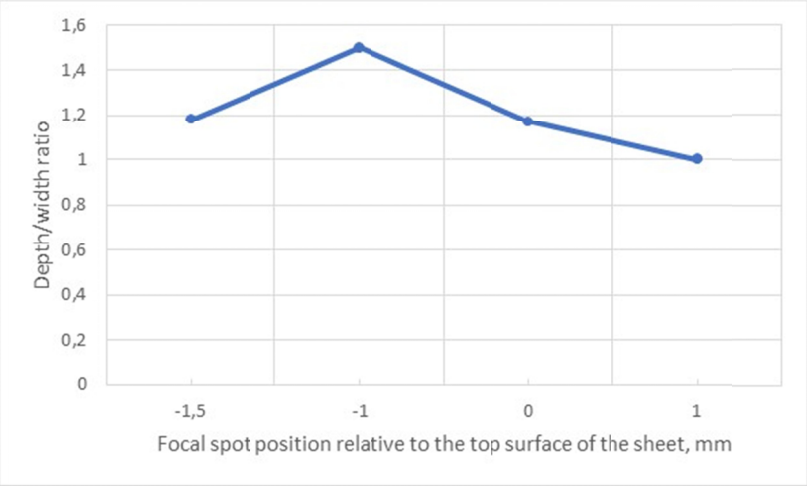

Fig. 8. Influence of the focal spot position on the depth/width ratio of the weld during bead-on-plate laser welding of 2.0 mm thick sheet of AISI 304 stainless steel at constant laser beam output power 1.0 kW and welding speed 1.5 m/min, Table 3

top surface is similar double-T configuration, Fig. 9. However, the depth/width ratio depends on the welding speed and energy input, and it is ranged in 1.5÷2.5 for the investigated range of parameters, as shown in Fig. 10. Due to the favorable shape of fusion zone the focal spot position 1.0 mm below the top surface of the 2.0 mm thick sheet (beam focused in the middle of the thickness, Fig. 8) was considered as optimal, and the test butt joints were produced at such focal spot position. However, in the case of butt joints the macrographs indicate clear displacement of the sheets, and also incomplete fusion of the joint No. 3, and single small pores in the weld metal of joint No. 1 and 2, Fig. 11. Nevertheless, the diameter of the single pores is less than 100 µm.

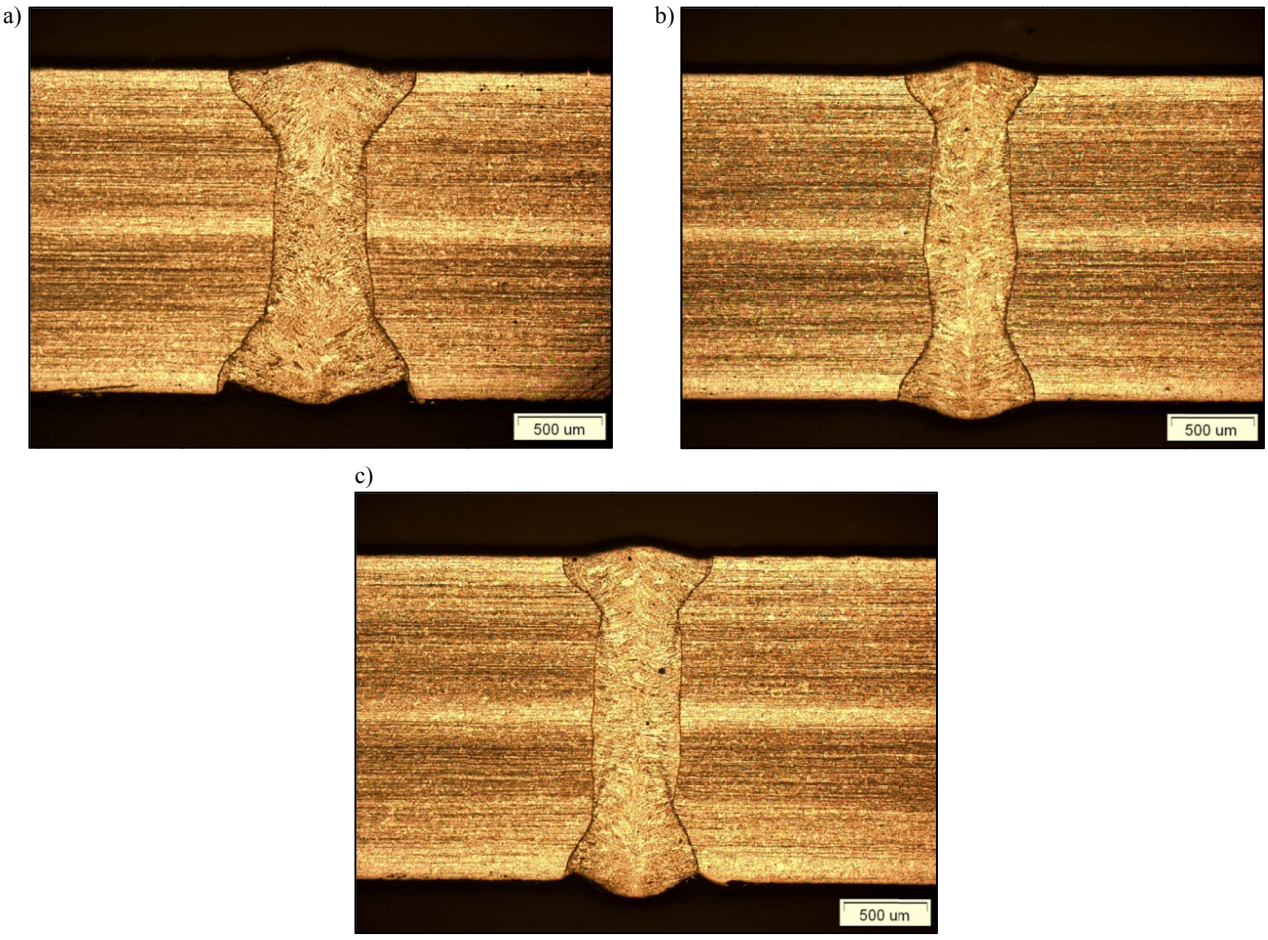

Fig. 9. Macrostructure on cross sections of the simulated welds produced on AISI 304 steel sheets 2.0 mm thick by bead-on-plate laser welding at constant focal spot positions 1 mm below the top surface and different energy inputs (Table 3); a) 30 J/mm (1.0 kW, 2.0 m/min), b) 22.5 J/mm (1.5 kW, 4.0 m/min), c) 20 J/mm (1.0 kW, 3.0 m/min)

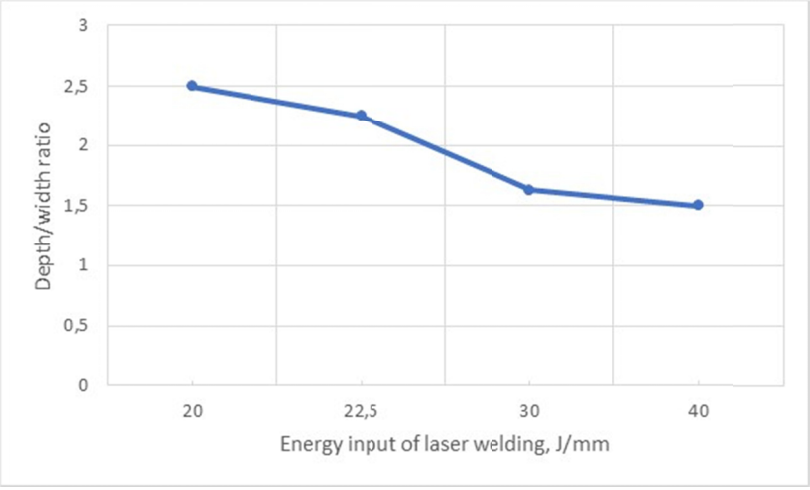

Fig. 10. Influence of the energy input of bead-on-plate laser welding of 2.0 mm thick sheet of AISI 304 stainless steel on the depth/width ratio of the weld (at focal spot positions 1 mm below the top surface), Table 3

The microstructure of the as-received (delivery condition) 2.0 mm thick sheet of stainless AISI 304 steel is shown in Fig. 12. As can be seen the micrograph exhibits strongly strained band microstructure which is characteristic after rolling deformation. Observations of the micrographs of the welds in the region of fusion line reveal that the width of the heat affected zone HAZ is negligible about a few microns. This is due to the high power density of the laser beam as a heat source but also due to relatively low thermal conductivity of the austenitic stainless steel.

In general, the fusion zone of the welds is composed of very fine dendritic grains. As can be seen in the Fig. 13 showing the microstructure of the weld produced at the highest heat input of

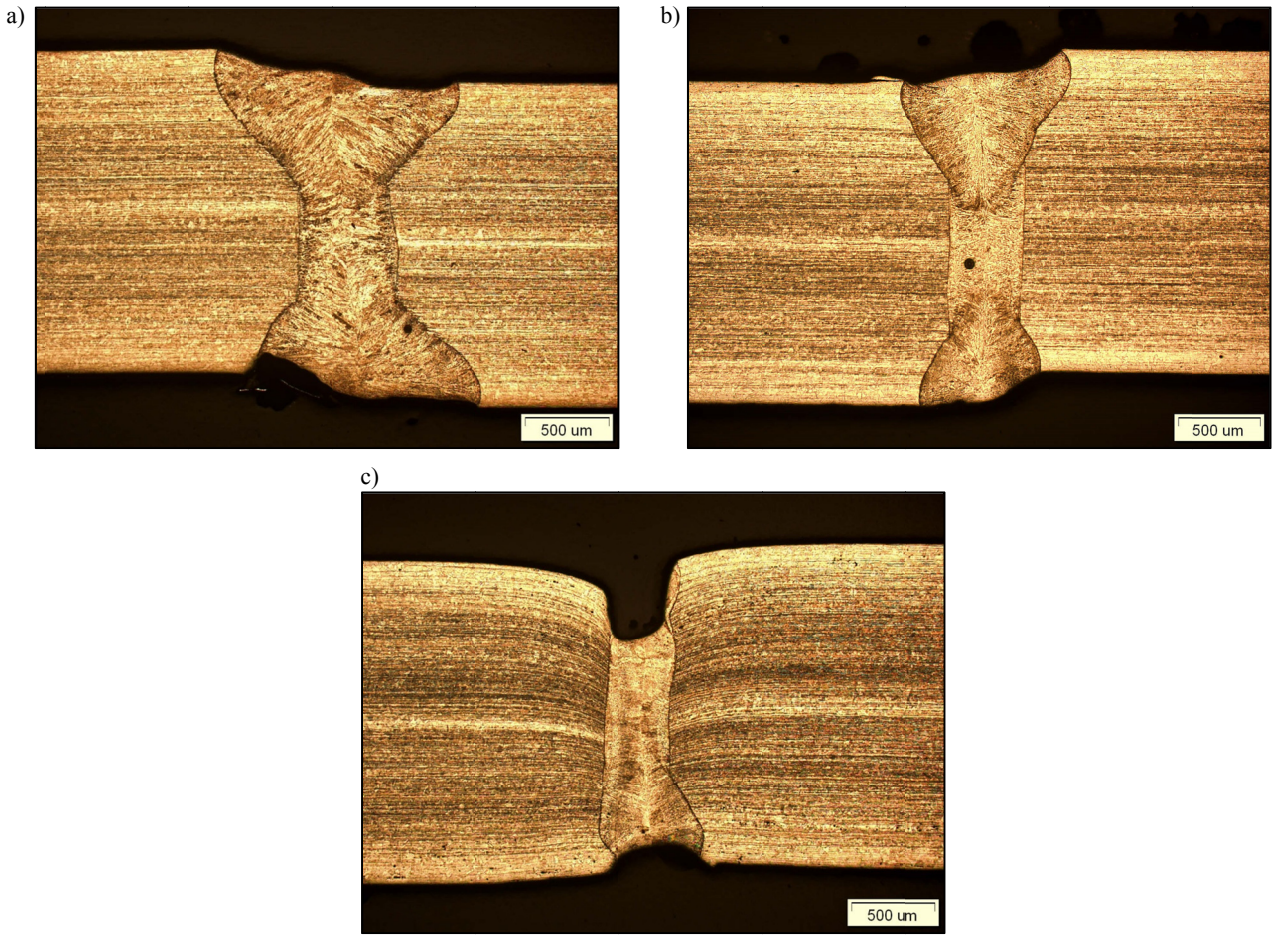

Fig. 11. Macrostructure on cross sections of butt joint of AISI 304 steel sheets 2.0 mm thick welded by the disk laser at different energy input (Table 3); a) 30 J/mm (1.0 kW, 2.0 m/min), b) 22.5 J/mm (1.5 kW, 4.0 m/min), c) 20 J/mm (1.0 kW, 3.0 m/min)

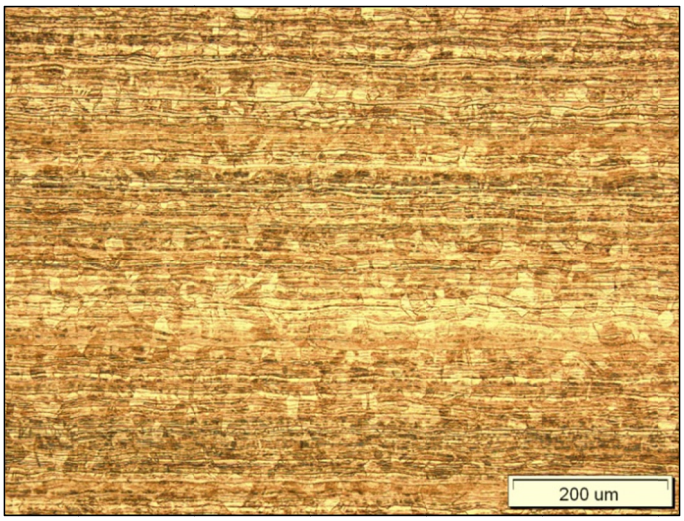

Fig. 12. Microstructure of the base metal AISI 304 steel sheets 2.0 mm thick

120 J/mm (laser power 1.0 kW and welding speed 0.5 m/min), along the fusion line partially melted grains from the side of base metal occur. From those partially melted grains, epitaxially grown columnar grains can be observed, which are perpendicular to the fusion line. Within those grains fine dendrites can be identified. The secondary arm spacing depends on the welding parameters, mainly laser output power and welding speed, thus heat input and related cooling rate of the weld metal. The direct observations of the fusion zone under scanning electron microscope (SEM) allowed to roughly estimate the secondary arm spacing. Thus, the estimated secondary arm spacing for the welds produced in the investigated range of parameters is approximately 5÷8 μm, indicating high cooling rates. The frontal surfaces of dendrites meet in the middle of the welds forming

the crystallization line, as can be seen on the cross section in Fig. 13a. Presence of the crystallization line may lead to deterioration of mechanical performance of the joints because impurities present in the alloy and eutectics with low-melting point may accumulate in this region.

Detailed observations of micrographs and analysis of the weld metal microstructure indicate that the microstructure is mainly austenitic (Feγ) with a small share of delta (Feδ) ferrite. It should be noted that the microstructure of the AISI 304 steel is austenitic in general. However, the single-phase austenitic microstructure may be obtained just under thermodynamic equilibrium conditions. Since the solidification of this type of steel, with the classic chemical composition, begins with the formation of δ-phase (L + δ) as the primary product of solidification, the ferrite delta may also occur in the microstructure, especially when the cooling rates are rapid, like during laser processing. The presence of delta ferrite in laser welded joints are also confirmed by other investigators, such as S. Katayama et al. [1]. The share of the delta ferrite is similar for all of the studied welds, so it can be concluded that the laser welding parameters in the investigated range have no significant influence on the microstructure of weld metal.

Microhardness measurements performed on the cross sections of the butt joints in the middle of the sheet thickness showed that the base metal of AISI 304 stainless steel exhibits microhardness in the range from 230HV0.1 to 250HV0.1, Fig. 15. While the microhardness in the fusion zone drops down below 200HV0.1, Fig. 15. The lowest drop in microhardness was observed in a case of the test joint welded at the lowest energy input of 20 J/mm (power of 1. kW, welding speed 3 m/min). In this case the distribution of microhardness bas very stable across the fusion zone at a level of 180÷195HV0.1, Fig. 15. On the other hand the butt joint welded at the highest energy input of 30 J/mm have shown most significant drop of microhardness ranged within 131÷159HV0.1, Fig. 15. So it is evident that the welding parameters, especially energy input affect the microhardness in the fusion zone thus mechanical properties of the joints. A significant decrease in hardness in the weld metal is

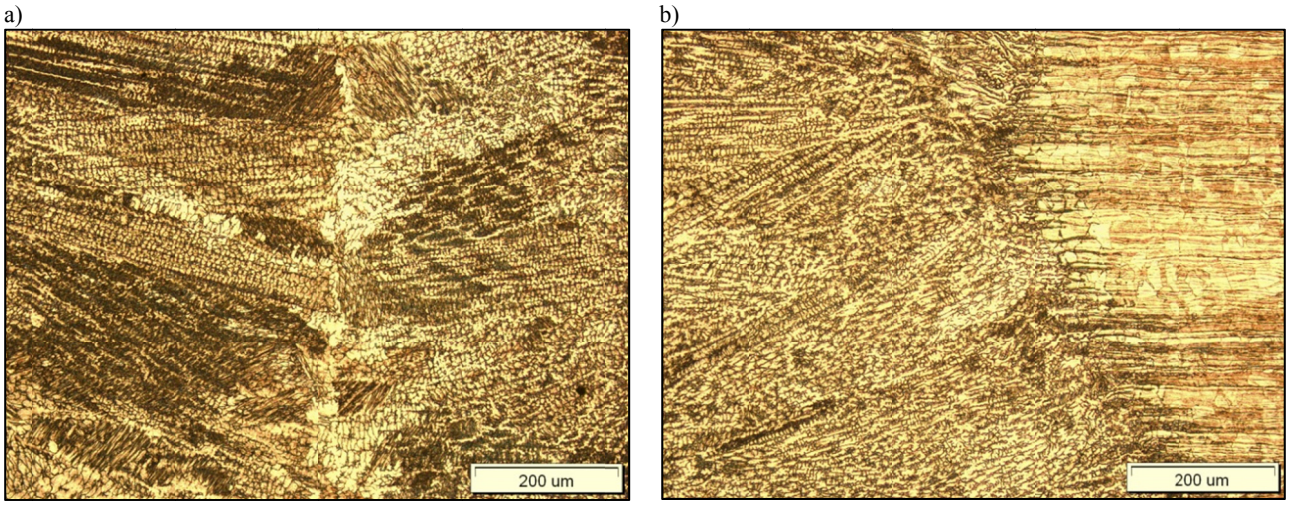

Fig. 13. Microstructure of the bead-on-plate weld No.1 on 2.0 mm thick sheet of AISI 304 stainless steel produced at the energy input 120 J/mm (Table 3); a) middle region of fusion zone, b) fusion line (from left weld metal, fusion line, HAZ)

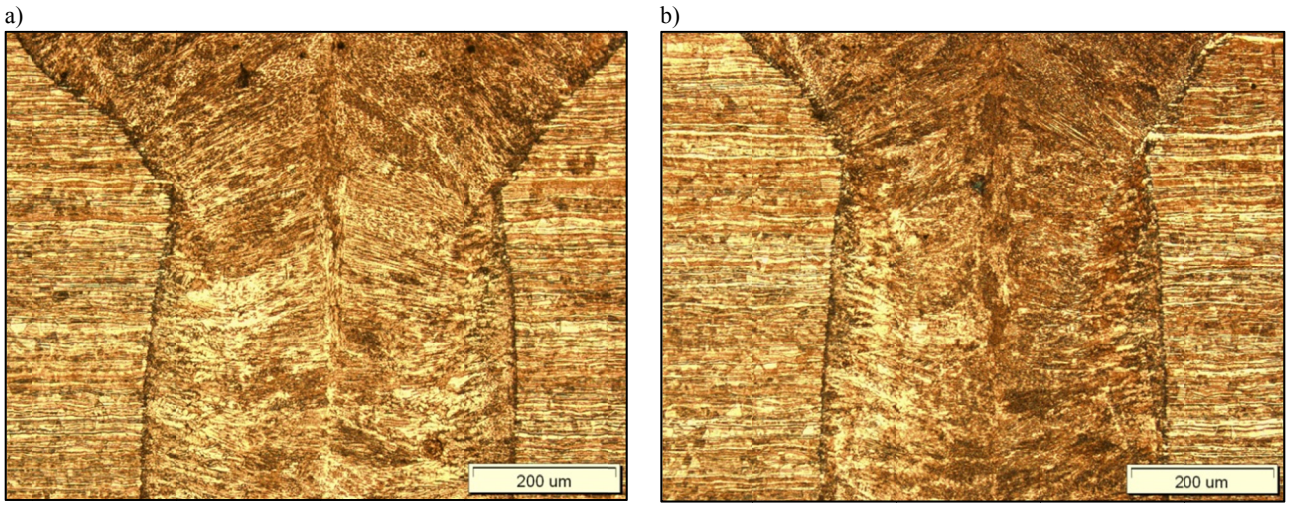

Fig. 14. Microstructure of the bead-on-plate welds on 2.0 mm thick sheet of AISI 304 stainless steel produced at different energy input (Table 3); a) bead No.9 (22.5 J/mm), b) bead No.8 (20 J/mm)

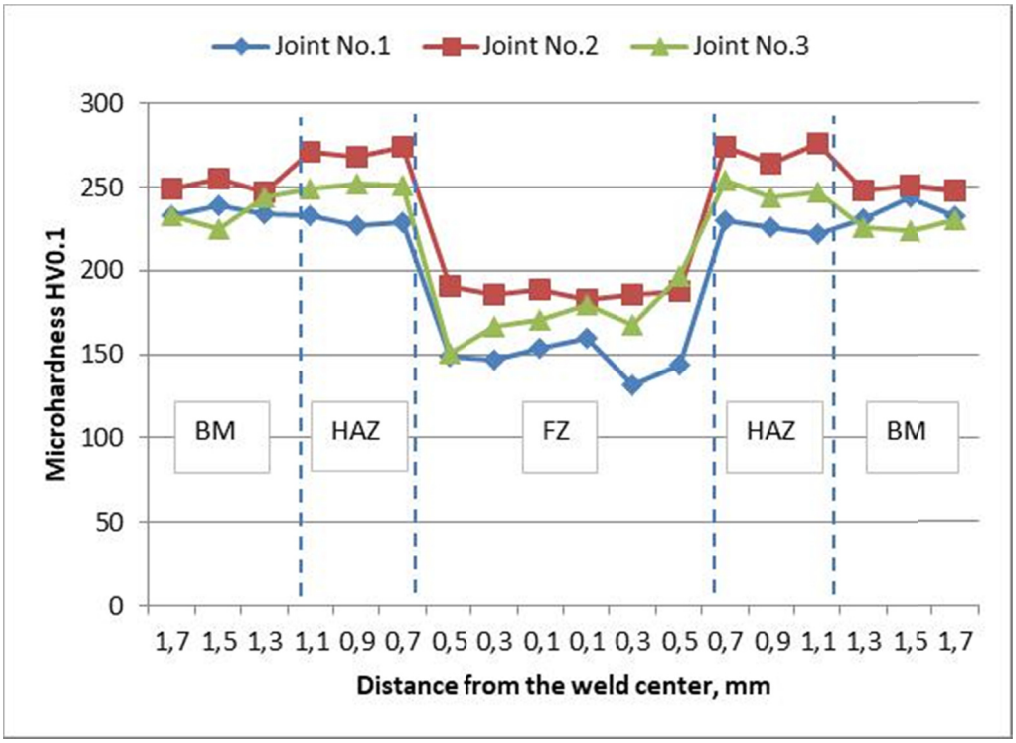

Fig. 15. Microhardness distribution on the cross section of butt joints of AISI 304 steel sheets 2.0 mm thick welded by the disk laser at different energy input (Table 3); a) Joint No.1, 30 J/mm (1.0 kW, 2.0 m/min), b) Joint No.2, 22.5 J/mm (1.5 kW, 4.0 m/min), c) Joint No.3, 20 J/mm (1.0 kW, 3.0 m/min)

unfavorable, as it will cause a reduction in mechanical properties of the welded joints. However, the base metal of AISI 304 stainless steel sheet was strain hardened after cold rolling. The melting and subsequent solidification of the welded material causes a loss of the strengthening effect. On the other hand the mainly single-phase austenitic steel is susceptible to grain growth during solidification and also during heat treatment. While the hardness and also mechanical properties are related to the grain size, low energy inputs of welding are beneficial because they lead to providing a fine-grained microstructure of welds. For this reason the weld metal of the joint produced at the highest energy input of 30 J/mm showed the lowest microhardness in the weld metal, as can be seen in Fig. 15.

4. Summary

The autogenous laser welding process of chrome-nickel type austenitic AISI 304 steel was investigated. The influence of basic process parameters and technological conditions on the weld quality and fusion zone configuration was determined. In the range of optimal parameters high quality welds can be produced with double-T configuration of the fusion zone and the depth/width ratio up to 2.5. The welds produced within optimal parameters exhibit very narrow HAZ and fine dendritic microstructure of the weld metal consisting of mainly austenite (Feγ) with a small share of delta (Feδ) ferrite. Microhardness of the investigated 2.0 mm thick sheets of AISI 304 steel is ranged in 230÷250HV0.1, while in the fusion zone clear drop of microhardness occur. The obtained results indicate that the drop of microhardness in the fusion zone is clearly related to the energy input of laser welding. The higher energy input of laser welding, the higher drop of microhardness in the weld metal.

REFERENCES

[1] H.M. Khalid. S. Katayama, Quarterly Journal of the Japan Welding Society **27** (2), 69 (2009), doi:10.2207/qjjws.27.69s.

[2] N. Kumar, et al., JOLT 88, 24-39 (2017).

[3] M.R. Ghusoon, et al., Metals **7**, 546 (2017). doi:10.3390/met7120546.

[4] A. Czupryński, Materiali in Tehnologije **51** (2), 205 (2017), doi:10.17222/mit.2015.165.

[5] A. Grajcar, M. Różański, M. Kamińska, B. Grzegorczyk, Materiali in Tehnologije **50** (6), 945 (2016), doi:10.17222/mit.2015.253.

[6] A. Lisiecki, A. Kurc-Lisiecka, Materiali in Technologije **51** (1), 29 (2017), doi:10.17222/mit.2015.160.

[7] A. Zieliński, G. Golański, M. Sroka, I. J. Press. Vess. Pitping **152**, 1 (2017), doi:10.1016/j.ijpvp.2017.03.002.

[8] A. Kurc-Lisiecka, Materiali in Tehnologije **51** (4), 643 (2017), doi:10.17222/mit.2016.234.

[9] L.A. Dobrzański, J. Madejski, W. Malina, W. Sitek, J. Mater. Process. Technol. **56** (1-4), 887 (1996), doi:10.1016/0924-0136(96)85119-3.

[10] W. Sitek, J. Trzaska, L.A. Dobrzański, Mater. Sci. Forum **575-578**, 892 (2008), doi:10.4028/www.scientific.net/MSF.575-578.892.

[11] L.A. Dobrzański, W. Sitek, J. Mater. Process. Technol. **89-90**, 467 (1999), doi:10.1016/S0924-0136(99)00140-5.

[12] T. Tański, K. Labisz, Z. Brytan, E. Jonda, M. Sroka, Procedia Eng. **74**, 429 (2014), doi: 10.1016/j.proeng.2014.06.294.

[13] T. Węgrzyn, J. Piwnik, A. Borek, A. Kurc-Lisiecka, Materiali in Technologije **50** (6),1001 (2016), doi: 10.17222/mit.2015.159.

[14] M. Burda, A. Gruszczyk, T. Kik, et al., Proceedings of ICEM 15, Experimental mechanics. New trend and perspectives, 411 (2012).

[15] A. Kurc-Lisiecka, J. Piwnik, A. Lisiecki, Arch. Metall. Mater. **62** (3), 1651 (2017), doi: 10.1515/amm-2017-0253.

[16] M. Bonek, Arch. Metall. Mater. **59** (4), 1647 (2014), doi:10.2478/amm-2014-0280.

[17] W. Pakieła, T. Tański, Z. Brytan, K. Labisz, Appl. Phys. A, **122**, 352 (2016), doi: 10.1007/s00339-016-9834-z.

[18] A. Lisiecki, Materiali in tehnologije **51** (4), 577 (2017), doi:10.17222/mit.2016.106.

[19] B. Szczucka-Lasota, B. Gajdzik, T. Węgrzyn, Ł. Wszołek, Metals **7** (9), 339 (2017), doi:10.3390/met7090339.

[20] K. Janerka, M. Pawlyta, J. Jezierski, J. Szajnar, D. Bartocha, J. Mat. Proc. Tech. **214** (4), 794 (2014), doi:10.1016/j.jmatprotec.2013.11.027.

[21] W. Tarasiuk, A.L. Gordienko, A. Wolocko, J. Piwnik, B. Szczucka-Lasota, Arch. Metall. Mater. **60** (4), 2939 (2015), doi: 10.1515/amm-2015-0469.

[22] M. Zuk, J. Gorka, A. Czuprynski et al., Metalurgija **55** (4), 613 (2016).

[23] B. Szczucka-Lasota, Arch. Metall. Mater. **61** (3), 1431-1436 (2016), doi: 10.1515/amm-2016-0234.

[24] A. Lisiecki, R. Burdzik et al., Arch. Metall. Mater. **60** (4), 2913 (2015), doi: 10.1515/amm-2015-0465.

[25] D. Hadryś, T. Węgrzyn, J. Piwnik, Arch. Metall. Mater. **61** (1), 123-126 (2016).

[26] G. Moskal, A. Grabowski, A. Lisiecki, Sol. St. Phenom. **226**, 121 (2015), doi:10.4028/www.scientific.net/SSP.226.121.

[27] D. Hadryś, Arch. Metall. Mater. **60** (4), 2525 (2015), doi: 10.1515/amm-2015-0409.

[28] A. Kurc-Lisiecka, A. Lisiecki, Materiali in Tehnologije **51** (2), 199 (2017), doi:10.17222/mit.2015.158.